



An assessment of height–diameter growth variation in an unmanaged *Fagus orientalis*-dominated forest

Charles P.-A. Bourque^{1,2} · Mahmoud Bayat³ · Chengfu Zhang⁴

Received: 16 August 2018 / Revised: 30 January 2019 / Accepted: 3 April 2019 / Published online: 10 April 2019
© Springer-Verlag GmbH Germany, part of Springer Nature 2019

Abstract

Allometric variations in tree height and stem diameter are a genetically controlled trait that reflects the ability of trees to adjust to different environmental conditions. This paper examines the ecological control of abiotic and forest-state variables on height- and stem diameter-growth in oriental beech (*Fagus orientalis* Lipsky) in an unmanaged, high-elevation forest of northern Iran. Spatially explicit abiotic variables of growing-season mean potential solar radiation, mean air temperature, topographic wetness index (TWI, as a proxy of soil water content) and wind velocity essential to the analysis were generated numerically by computer models. Forest-state variables of total tree height (H) and diameter at breast height (D) and stand basal area (BA) were assessed at individual sample plots. Degree of explanation of observed variation in individual-tree H and plot-level changes in stem D (i.e. dD/dt) by the assemblage of modelled abiotic and observed tree variables was 87.4%, with a root mean squared error (RMSE) and mean absolute error (MAE) of 3.60 and 2.84 m and 67.3%, RMSE = 0.13 cm and MAE = 0.10 cm, respectively. Wind velocity, TWI and mean air temperature provided the greatest overall influence on the calculation of static H and annual D -increment, with relative impact of 38.3, 37.3 and 9.6 and 7.7, 6.4 and 6.7, respectively. The other variables, including BA, had weak to no control on tree-growth response. Methods used here are sufficiently general to address tree-growth response in many other tree species around the world, with or without changes to site conditions.

Keywords Abiotic and biotic controls · Competition · Computational fluid dynamics · Permanent sample plots · Topographic wetness index · Wind velocity

Introduction

Being able to quantify tree growth spatially and over time is central to the management of forests worldwide. Tree growth is largely controlled by the prevailing stand abiotic and biotic

conditions (Goudriaan 1977; Oliver and Larson 1996; Bonan 2008; Byun et al. 2013), including (1) available solar radiation, atmospheric and soil temperatures, wind velocities, soil water and nutrient content (Spurr and Barnes 1980; Botkin 1993; Oliver and Larson 1996; Kimmins 1997; Bourque et al. 2000) and (2) factors affecting inner-stand structure, competition and growing potential of individual trees (Weiskittel et al. 2011), including vertical stand composition, tree spacing, basal area (BA; Kahnmoie 2003; Coomes and Allen 2007; Watt and Kirschbaum 2011; Weiskittel et al. 2011; Huang et al. 2013; Mohammadi et al. 2018) and tree size.

Changes in tree growth allocation to height (H) and stem diameter (D) are a complex physiological, genetically programmed process (Becker et al. 2000; Jiang et al. 2016) that reflects the ability of trees to adapt to variable environmental conditions (Henry and Aarssen 1999; Koch et al. 2004; Poorter et al. 2006; King et al. 2009; Jiang et al. 2016). Trees have been documented to allocate their annual stem growth to H growth whenever resources are abundant and competition for sunlight places a greater significance on H

Communicated by Arne Nothdurft.

✉ Mahmoud Bayat
Mbayat@rifr-ac.ir

¹ Faculty of Forestry and Environmental Management, University of New Brunswick, 28 Dineen Drive, PO Box 4400, Fredericton, NB E3B 5A3, Canada

² School of Soil and Water Conservation, Beijing Forestry University, 35 East Qinghua Road, Haidan District, Beijing 100083, China

³ Research Institute of Forests and Rangelands, Agricultural Research, Education and Extension Organization (AREEO), Tehran 13185-116, Iran

⁴ Ecology and Environmental College, Inner Mongolia Agricultural University, Hohhot 010018, Inner Mongolia, China

than on D growth (Koch et al. 2004; Falster and Westoby 2005; Watt and Kirschbaum 2011; Harja et al. 2012; Trouvé et al. 2015). As trees continue to grow to maturity, annual H growth decreases in consecutive years mainly as a response to increases in hydraulic resistance and lowering of transpiration and photosynthetic capacity in taller trees (Oliver and Larson 1996; Ryan and Yoder 1997; Hubbard et al. 1999; Becker et al. 2000; Koch et al. 2004; Bonan 2008). Static H – D ratios in heterogeneous landscapes have also been known to vary with prevailing wind conditions, commonly decreasing with increasing wind speeds (Thomas et al. 2015). Increased swaying in tall trees triggers a predominance in improved radial growth at the expense of H growth in order to preserve the biomechanical stability of the stem (Meng et al. 2006).

In general, characterising stand conditions over large sections of landscapes is extremely difficult with field measurements alone, as the measurements may be taken far apart from each other in both space and time. Biotic variables suggestive of forest state, e.g. stand BA and density and individual tree H and D , are taken sporadically across the landscape, as most existing operational forest-monitoring networks have been created to answer forestry-related questions (for forest-management reasons) for regions spanning hundreds of thousands to millions of hectares (ha), as is common in North America, Russia and other parts of the world. Direct measurements of abiotic variables in situ are rarely included in such data captures. For this reason, capturing variability in forest landscapes at moderate spatial resolutions presents a major challenge. For this reason, combining forest plot data with computer-generated results of abiotic variables by means of evolutionary programming algorithms (machine learning) provides opportunities to advance our assessment, predictive capabilities and understanding of forest growth in heterogeneous landscapes at spatial resolutions relevant to on-the-ground operations common to forest and land management interests (< 100 m).

In recent years, there have been many attempts to describe abiotic attributes of landscapes by numerical methods (e.g. finite-difference modelling, artificial neural networks and spatial interpolation) and relate their values at point locations to tree growth measured in the field. Examples of analyses relating tree-growth, plot-level or photo-interpreted forest-cover descriptions to modelled abiotic quantities include those of Austin et al. (1996), Lebourgeois et al. (2005), Hassan and Bourque (2009), Byun et al. (2013), Ashraf et al. (2013), Baah-Acheamfour et al. (2013), Detto et al. (2013) and Bourque and Bayat (2015). Level of agreement between modelled and observed data generally varies with spatial resolution of the digital elevation model (DEM; Ashraf et al. 2012) and forest-cover data used in the analysis.

The principal objective of this study was to examine the abiotic and biotic controls on tree H - and stem D -growth and

related patterns of H – D allometry in a heterogeneous, beech-dominated forest. Spatial patterns in beech development over a 9-year growing period, from 2003 to 2012, were related to (1) point extractions from computer-generated surfaces of growing-season mean potential solar radiation, seasonal mean air temperature, topographic wetness index, in representing variation in soil water and nutrient content and estimates of wind velocity generated with a computational fluid dynamics model (CFD) and (2) associated field measurements of tree H and D and plot BA (based on 2003 data) with the assistance of a system of simultaneous differential equations of tree growth and symbolic regression (Schmidt and Lipson 2009). The latter element is used in formulating species-specific functions of asymptotic tree H (i.e. H_{\max} , a site indicator of growth potential; Falster and Westoby 2005; Poorter et al. 2006; Banin et al. 2012) and cumulated leaf area. Tree leaf area is an important indicator of photosynthetic capacity in living trees (Thomas and Bazzaz 1999).

Methods

Study area and plot network

In northern Iran, the Hyrcanian (Caspian) forest covers approximately 50,000 km², including the provinces of Golestan, Mazandaran and Gilan (Marvie-Mohadjer 2012; Fig. 1). Due to its humid, temperate climate and fertile soils, this region is renowned for its high forest productivity. Intensive human settlement in the lower elevations, as early as 1100 AD, has left large portions of the lowlands void of forest cover (Sefidi et al. 2011; Jaafari et al. 2014).

Beech forests in this region (Bayramzadeh et al. 2012) are mixed with *Carpinus betulus*, *Alnus subcordata*, *Acer velutinum* and several other tree species and shrubs. These forests are mostly broadleaved, but *Taxus baccata* and *Cupressus* spp. do appear on some specialised sites (Marvie-Mohadjer 2012). Close-to-nature silviculture (a management system based on small-scale interference and tree-group selection) is the harvesting method currently practiced in the region. It is similar in principle to forest-ecosystem management practiced in North America (Patry et al. 2013). This forest-management approach is best suited for establishing and maintaining mixed forests (Leibundgut 1983; Otto 1993a, b; Bayat et al. 2013) and permanent forest cover (Heyder 1986; Marvie-Mohadjer 2012).

The experimental forest (Kheyroud forest) is an 80-km² unmanaged compartment of the greater Hyrcanian forest located about 7 km east of the port city of Nowshahr (36°39'N, 51°30'E; 7.5 m above mean sea level, AMSL; Fig. 1a). The northern lower boundary of the Gorazbon section, one of eight sections of the Kheyroud forest and location of the plot network (Fig. 1a), sits at roughly 1010 m

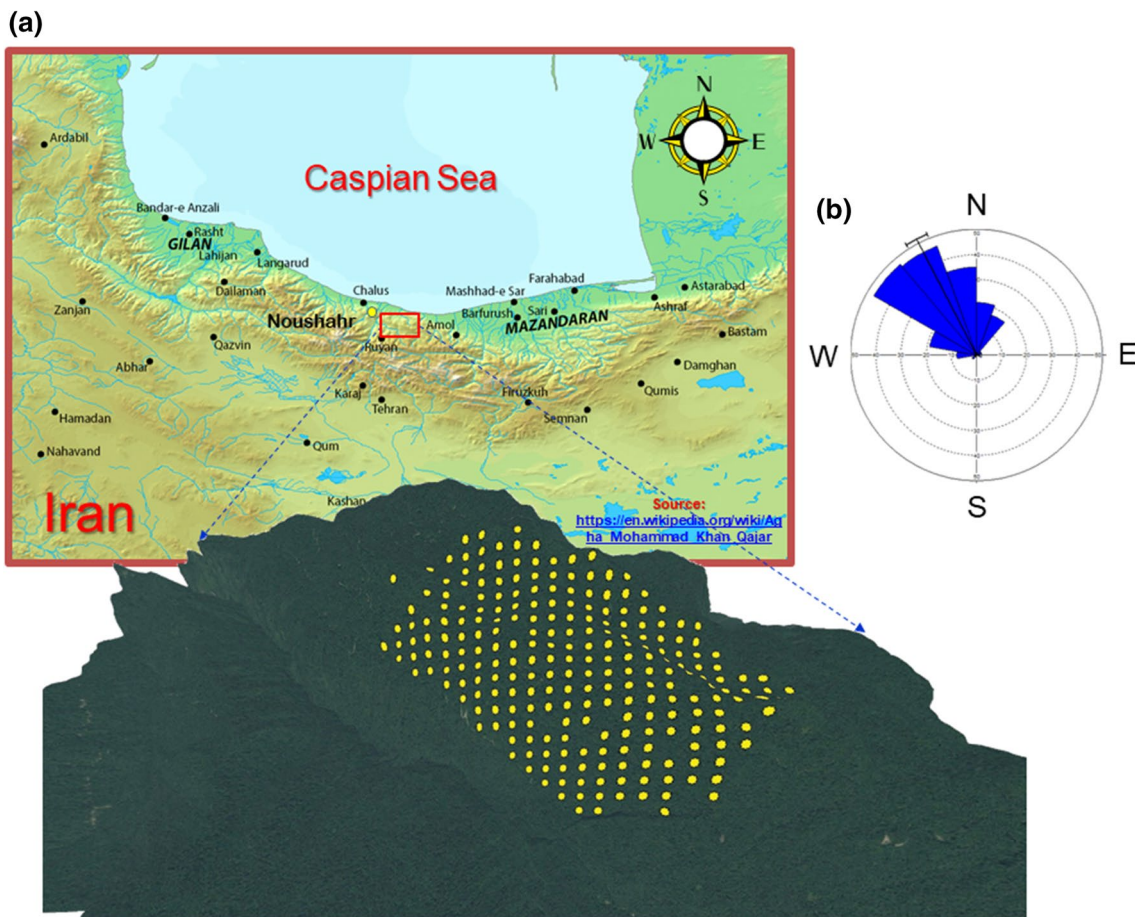


Fig. 1 Forest plots essential to the current beech-growth study (a) close to Nowshahr, Iran. Also, indicated are the growing-season (April–October) wind directions recorded at the Nowshahr climate

station (b); mean wind direction and standard deviation are indicated as a solid line at 333° from true North (0°) and error bar

AMSL; the section's highest elevation lies at about 1380 m AMSL. The Kheyroud forest consists of 80 different tree species and 50 shrub species at various densities. Mean annual precipitation in the area is about 1303 mm based on data from 1985 to 2008, with October and August, respectively, being the wettest (235 mm) and driest month (42 mm) of the year. Mean annual air temperature is 16.2 °C, with February and August being the coldest (7.1 °C) and warmest months (25.1 °C). Mean annual pan evaporation is about 1031 mm, with highest average monthly evaporation occurring in August (155.4 mm) and lowest, in January (26.2 mm). Following the soil-taxonomic system of the United States Department of Agriculture, soils in the area are classified as highly productive udic alfisols. Organic matter accumulation on the forest floor is usually > 5 cm (Namiranian 2009).

The plot network in the Gorazbon section is designed on a rectangular grid (150 m × 200 m) and consists of 258 fixed circular plots of 0.1 ha each (Fig. 1a; Namiranian 2009), with 176 containing predominantly oriental beech and having GPS (global positioning system) coordinates

for geo-referencing. Stem D measurements were taken with calipers in both 2003 and 2012 for all living stems of all tree species with a diameter > 7 cm. A collection of tree H were also made in 2003 on a sub-sample of beech trees (accounting for about 10.5% of 2246 sampled trees), with no follow-up measurements in 2012. Figure 2 describes the actual plot-level change in quadratic mean diameter at breast height of oriental beech (DBH and $\Delta\text{DBH} \pm$ standard deviation) as a function of plot location (Fig. 2a) and DBH (or D ; Fig. 2b).

Tree-growth equation development

Here, we estimate individual-tree growth with respect to a coupled system of differential equations for tree H (m) and stem D (cm). The former equation is based on a differentiation of a static H -equation explicitly relating tree H to stem D . The D -increment equation predicts annual stem expansion anticipated under optimal-to-sub-optimal conditions as site-biophysical conditions (e.g. incident solar radiation, wetness index, seasonal air temperature and wind velocity) vary in

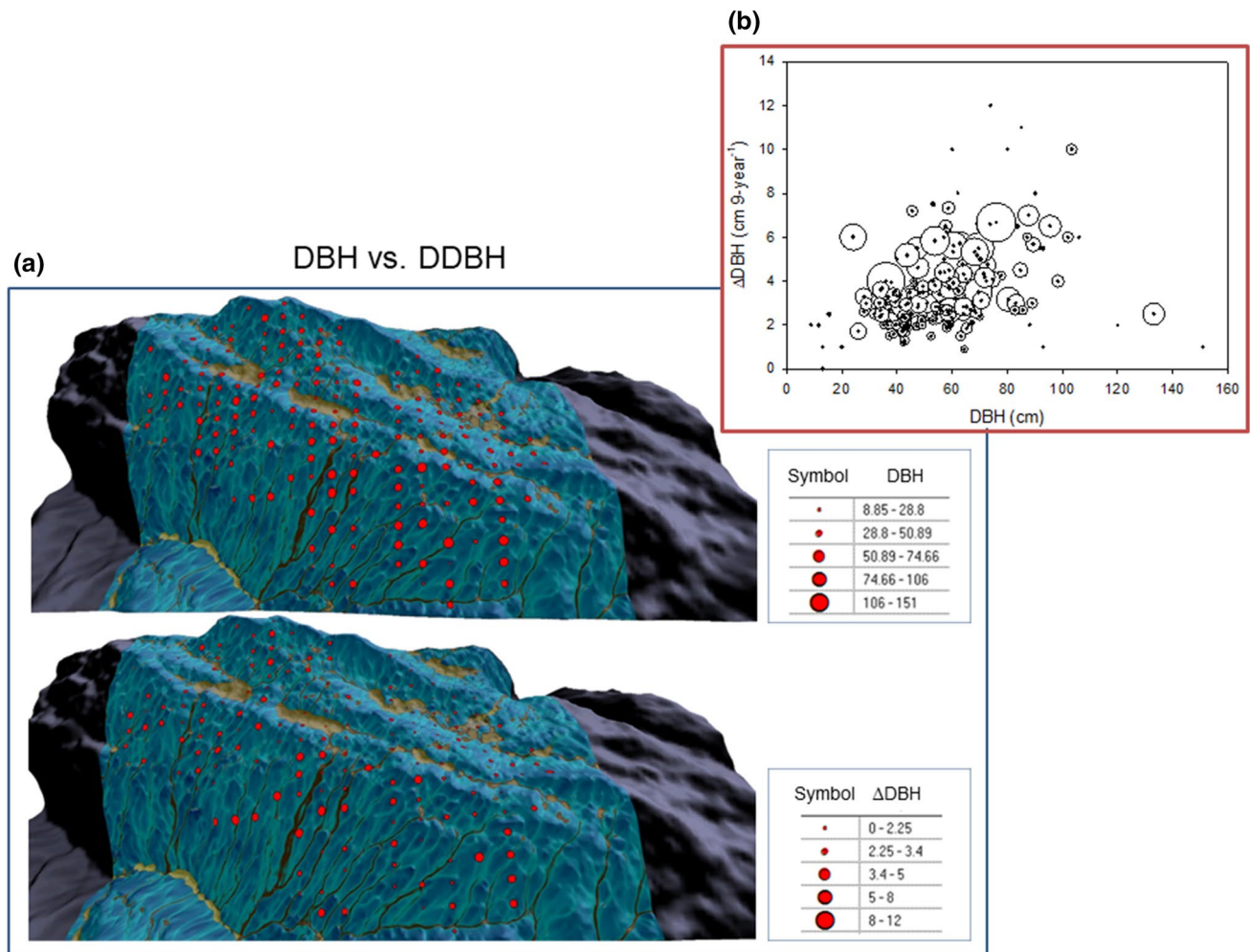


Fig. 2 Actual plot variation in quadratic mean diameter at breast height (DBH or D , in cm) and DBH (D)-increment (Δ DBH) for the study area (a). Background colours (shades of blue to cyan colours and browns) vary according to variation in a SAGA-based calculation of topographic wetness index (TWI, non-dimensional) for the plot-network-area in the Gorazbon section forest. Brown colours on the high-elevation plateau coincide with land depressions (vernal pools),

where water has an opportunity to pool during the snowmelt season, i.e. TWI~16. Low values (blue colour) coincide with drier soil conditions. A comparative graph of Δ DBH and DBH is provided in the inset (b). The circles around the individual points (quadratic mean diameter) are proportional to the standard deviation associated with individual-tree measurements. Isolated points, without circles, are associated with single tree measurements. (Color figure online)

space, given tree size (i.e. tree H and stem D) and leaf area. The two rate equations are linked through the asymptotic maximum tree H or H_{\max} .

The core assumption here is that as trees grow, the cost of maintaining a given volume of living tissue increases. As a result, the negative cost associated with growth causes tree growth to decelerate as trees get larger (Oliver and Larson 1996). Volume growth for unconstrained conditions, defined either as dV/dt or $d[D^2H]/dt$, can be expressed as a differential equation of the continuous logistic function, such that

$$\frac{d[D^2H]}{dt} = G \cdot La \left(1 - \frac{DH}{D_{\max}H_{\max}} \right) \quad (1)$$

(Botkin et al. 1972), where G is the intrinsic growth rate (cm^3 of wood volume per m^2 of leaf area), La is the cumulated leaf area (m^2) and H_{\max} and D_{\max} are the maximum possible tree H (m) and stem D (cm) achievable under prevailing site conditions (Botkin et al. 1972).

Tree H is modelled as a function of stem D and a site-specific (pixel) calculation of H_{\max} . A three-parameter cumulative (asymptotic) Weibull function is used to model tree H at breast height (i.e. 1.3 m above the ground surface), such that

$$H = 1.3 + H_{\max} [1 - \exp(-b_1 D^{b_2})] \quad (2)$$

(Weiskittel et al. 2011; Ahmadi et al. 2013; Thomas et al. 2015; Ahmadi and Alavi 2013) where b_1 and b_2 are equation coefficients that determine the shape of the H -function as a

function of D . The cumulative Weibull function is flexible and mathematically defined at its origin, i.e. $D=0$, whenever $H \leq 1.3$ m.

Given variable site conditions spatially in terms of incident solar radiation (SOL, kJ m^{-2}), topographic wetness index (TWI, non-dimensional), seasonal mean air temperature (T , $^{\circ}\text{C}$), wind velocity (WS, m s^{-1}) and basal area (BA, $\text{m}^2 \text{ha}^{-1}$), we express the impact of site conditions on D -growth as a logistic function of site-biophysical variables to give a new site and plot-specific calculation of H_{max} . Output from the logistic function, i.e. $\text{logistic}[f(x)] \rightarrow f(x) = 1.0 / \{1.0 + \exp[-f(x)]\}$, where “ x ” can be any number of independent variables, varies from 0.0 to 1.0 as site conditions for oriental beech vary from optimal to sub-optimal. Maximum tree H in Eq. (2) (i.e. H_{max}) is, thus, defined as

$$H_{\text{max}} = b_3 \text{logistic}\{f_1[\text{SOL}, \text{TWI}, T, \text{WS}, \text{BA}]\}, \quad (3)$$

where b_3 is an equation parameter set during regression that defines the highest possible H oriental beech may reach under optimal growing conditions. Expansion of the left-hand side of Eq. (1) and differentiation of Eq. (2) with respect to time give

$$2DH \frac{dD}{dt} + D^2 \frac{dH}{dt} = G \cdot \text{La} \left(1 - \frac{DH}{D_{\text{max}}H_{\text{max}}} \right), \quad \text{and} \quad (4)$$

$$\frac{dH}{dt} = H_{\text{max}} b_1 b_2 D^{b_2-1} \exp(-b_1 D^{b_2}) \cdot \frac{dD}{dt}. \quad (5)$$

Since long-term biophysical conditions across the landscape are, for now, considered static, H_{max} as defined in Eq. (3) can be treated as a constant in the differentiation of Eq. (2). Substituting Eq. (5) into Eq. (4) and solving for dD/dt give

$$\frac{dD}{dt} = \frac{G \cdot \text{La} (1 - DH / D_{\text{max}}H_{\text{max}})}{H_{\text{max}} b_1 b_2 \cdot D^{b_2+1} \exp(-b_1 D^{b_2}) + 2DH}. \quad (6)$$

Analogous to H_{max} in Eq. (2), leaf area (La) in Eq. (6) is assumed to vary as a logistic function of site-biophysical variables, i.e.

$$\text{La} = \text{La}_{\text{max}} \text{logistic}[f_2(\text{SOL}, \text{TWI}, T, \text{WS}, D, H - 1.3)], \quad (7)$$

where La_{max} represents the upper limit in attainable leaf area, similar to b_3 in Eq. (3). Combining the different equations, Eq. (6) can be rewritten as

$$\frac{dD}{dt} = \frac{G \cdot \text{La}_{\text{max}} (1 - D(H - 1.3) / \langle D_{\text{max}} b_3 \text{logistic}\{f_1(X)\} \rangle)}{\langle 100 \cdot b_3 \text{logistic}\{f_1(X)\} \rangle b_1 b_2 D^{b_2+1} \exp(-b_1 D^{b_2}) + 2 \cdot 100 \cdot D(H - 1.3)} \times \text{logistic}[f_2(Y)], \quad (8)$$

where arrays “ X ” and “ Y ” involve variables SOL, TWI, T , WS and BA and SOL, TWI, T , WS, D , BA and H from breast height (above 1.3 m), respectively; “100” in the denominator converts metres into cm.

Abiotic surface development

Key to the development of the abiotic surfaces is the DEM of part of the terrain including the plot network (Fig. 1). DEM data are derived from the Shuttle Radar Topography Mission one arc-second (~ 30 -m) Global DEM (<https://lta.cr.usgs.gov/SRTM1Arc>, last accessed on May, 2016), interpolated to 1-m resolution. Description of individual abiotic (environmental) surfaces (Fig. 3) and their derivation are as follows:

Solar radiation

Available solar radiation alters tree growth and tree distribution differently for different species. (Oliver and Larson 1996; Kimmins 1997). Sensitivity of oriental beech seedlings and saplings to various levels of incident solar radiation changes as plants mature (Tabari et al. 2005).

Incoming solar radiation in this study (Fig. 3a) is evaluated as a function of (1) DEM-based calculations of slope, aspect, view factor, horizon angle and terrain configuration factors, (2) sun-earth geometry and solar-illumination angles and (3) solar-flux calculations at the top of the atmosphere, based on calculations with the LanDSET (Landscape Distribution of Soil Moisture, Energy and Temperature) model of Bourque and Gullison (1998) and Bourque et al. (2000). Incoming sunlight at the top of the atmosphere is partitioned into its direct and diffused components as a function of incident angle, and each is handled differently as they pass through the atmosphere and interact with the underlying terrain, before being summed at the surface (Bourque and Gullison 1998). Many geographic information systems (commercial and open-sourced) have built-in subroutines to calculate cloud-free solar radiation spatially, including ERSI’s ArcGIS and System for Automated Geoscientific Analyses, or SAGA (Conrad et al. 2015).

Seasonal air temperature

Plant metabolism and growth increases with temperature (Nilsen and Orcutt 1996). For this reason, plant growth relates fairly well to indices of annual heat inputs. In this study, we use the growing-season mean air temperature as an index of growing-period heat input.

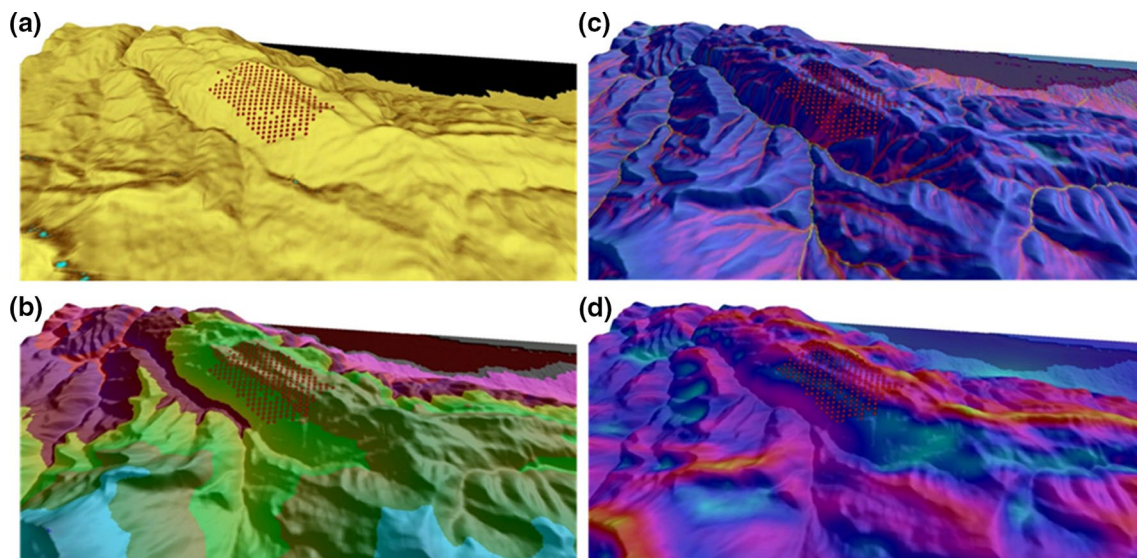


Fig. 3 Growing-season distributions of mean abiotic conditions; different colours are associated with spatially varying intensity of the variable. Distributions include **a** growing-season mean incident solar radiation ($\text{kJ m}^{-2} \text{days}^{-1}$), **b** near-surface air temperature ($^{\circ}\text{C}$), **c** SAGA-based calculation of topographic wetness index (non-dimensional) and **d** wind velocity (m s^{-1}). At the centre of each image is the network of forest plots, given for reference. Intensity of solar radiation varies from dark yellow (low intensity; $\sim 4.3 \text{ kJ m}^{-2} \text{days}^{-1}$) to lighter yellow (higher intensity; $\sim 8.6 \text{ kJ m}^{-2} \text{days}^{-1}$). Air temperature

drops from mean sea level ($\sim 21.1^{\circ}\text{C}$) to $\sim 2200 \text{ m AMSL}$ as a function of environmental lapse rate (i.e. $6.5^{\circ}\text{C km}^{-1}$). The pink in (c) represent wetter areas of the landscape, either as a result of the presence of wetlands, pools or low-ordered streams; the blues represent drier areas. The cyan and yellow in (d) represent areas of the landscape that are subject to low ($\sim 0.1 \text{ m s}^{-1}$) and high wind velocities ($\sim 13 \text{ m s}^{-1}$); areas with intermediate wind velocities are in pink and purple

Seasonal distribution of air temperature (Fig. 3b) is based on decreasing the growing-season (April–October) mean air temperature at Nowshahr station (i.e. 21.2°C ; based on data collected from 1977 to 2005) as a function of DEM elevation and an assumed mean environmental lapse rate of $6.5^{\circ}\text{C km}^{-1}$ over land (Merriam 1992). The environmental lapse rate describes the long-term averaged drop in air temperature with increased elevation (Lutgens and Tarbuck 1998).

Topographic wetness index

Tree species differ in their soil water requirements and tolerances (Oliver and Larson 1996). As soil information and precipitation patterns for the study area were not available, we elected to represent soil water distribution as a function of TWI (Fig. 3c). Production of surfaces of TWI as proxies of soil water (and soil nutrient) distribution is justified, as precipitation and thus soil water are spatially redistributed by topography and accordingly surfaces of TWI can be developed from DEM-height data alone (Beven 1997; Maathuis 2006; Gruber and Peckham 2008). Topographic wetness index considers steady-state (long-term) conditions and spatially uniform soil–water infiltration and transmissivity. There are many methods available to calculate TWI. For specific information on these methods, refer to Gruber and Peckham (2008) and routines available in SAGA. In

this study, we calculate the upslope contribution area in the calculation of TWI with the mass-flux method available in SAGA (Jaafari et al. 2018).

Wind velocity

An equally important abiotic variable affecting plant production is wind (Wadsworth 1959; Retuerto and Woodward 1992; Smith and Ennos 2003; Willoughby et al. 2009; Bang et al. 2010; Thomas et al. 2015). Wind velocities can have both positive and negative effects on plants, both from a physiological or biomechanical standpoint (Goudriaan 1977; Retuerto and Woodward 1992; Bang et al. 2010).

Wind is usually not considered in plant-growth studies, because of the difficulty in approximating its velocity and direction spatially. In this study, we use a CFD simulator to model wind flow over complex terrain (Fig. 3d), as specified by the DEM. The model solves the full 3-dimensional Navier–Stokes equations, which include the effects of atmospheric turbulence and thermal processes (Lopes 2003). Model calculations are based on a boundary-fitted coordinate system. Initial boundary conditions are specified by (1) the growing-season mean surface air temperature (the same as before) and wind velocity and direction (i.e. 1.7 m s^{-1} and 333° from true North; Fig. 1b) based on Nowshahr station climate records (1977–2005) and (2)

an assumed wind velocity of 6 m s^{-1} at 500 m AMSL. In the calculations, atmospheric temperature stratification is assumed neutral (i.e. $9.86 \text{ }^\circ\text{C km}^{-1}$), a common state of the planetary boundary layer under windy and cloudy daytime conditions (Geiger 1965).

Surface verification

As it requires vast amounts of field data to verify computer-generated surfaces at enhanced spatial resolutions (i.e. at 1-m resolutions), verification at this level is usually not possible. Satellite data could be used to verify some of these images (in particular, incident solar radiation and air temperature), but not at the current spatiotemporal resolution without extensive image-data preparation and processing. Topographic wetness index and wind velocity are more challenging to quantify directly, in view of their undetectable characteristics. Satellite-derived soil water distribution could be used to verify TWI, but deriving soil water content from space is especially problematic under fully developed canopies as is present in the area. Albeit the lack of verification, we expect that the modelled abiotic surfaces provide reasonably realistic descriptions of the long-term physical conditions of the Gorazbon forest area.

Symbolic regression and application

Symbolic regression is founded on an evolutionary search (genetic programming) of algebraic equations that describe trends in training data. The search is directed with the minimisation of differences between target values and values calculated with the equations generated with the procedure (Schmidt and Lipson 2009). Different from traditional regression that determines coefficients of known equations, no specific mathematical expression is needed as a beginning point. Instead, primary expressions are formed by randomly combining base functions of input variables (linear or nonlinear) with numerical operators. Equations retained by the approach are those that replicate the target output data the best; undesirable solutions are simply discarded. The search for equations ends whenever the desired accuracy in training-data replication or machine learning has been reached, i.e. lowest Akaike information criterion (AIC).

Abiotic conditions (Fig. 3) at forest-plot locations were summarised separately as averages of values falling within individual 0.1-ha plots. For every plot containing beech (176, in all), plot records comprised of mean values of all abiotic variables, plot BA and individual-tree H and stem D of 217 trees and average annual stem D -increment (dD/dt or $\Delta D/\Delta t$ in its discretised form) over the nine-year growing period (2003–2012). Development of the coupled system of differential equations of tree growth (H and D) followed a two-step process (Fig. 4). The first step addressed the

parameterisation of H (Eq. 2) and symbolic expansion of H_{\max} (i.e. Eq. 3) at the individual-tree-level given input of H and D (collected in 2003) and plot averages of modelled abiotic variables and stand BA (Table 1). The second step dealt with the development of the leaf-area component of Eq. (8) through symbolic expansion of Eq. (7) and specification of La_{\max} . Expansion of Eq. (7) was done within Eq. (8) and guided by plot-level estimates of D -increment, D (quadratic mean diameter at breast height), BA and H (modelled with an expansion of Eq. (2) obtained in step one, Fig. 4) and plot-means of the four abiotic variables. Parameters common to both differential equations (i.e. b_1 , b_2 , b_3 and H_{\max}) were determined during the parameterisation and symbolic expansion of H and H_{\max} in step one of the procedure (Fig. 4 and Table 1). Numerical integration of the coupled system of differential equations (i.e. expansions of Eqs. (5) and (8)) was performed with a fourth-order Runge–Kutta integration of tree H and D with a 0.00125-year timestep, i.e. from 2003 over a 9-, 25- and 80-year time horizon.

Results and discussion

Equation set development and performance statistics

Figure 5 provides a comparison of modelled and measured individual-tree H 's (2003) as a function of measured stem D 's. Overall explanation of variation in tree H with the fully parameterised version of Eq. (2) was 87.4%, with a root mean squared error (RMSE) and mean absolute error (MAE) of 3.60 and 2.84 m, respectively. Numerically based assessments of wind velocity and TWI across the study area provided the greatest overall impact on the calculations of H in oriental beech, with relative impact $\left[\text{i.e.} \left(\frac{\sum_{i=1}^{i=n} |\partial z / \partial x|}{n} \right) \cdot \sigma(x) / \sigma(z) \right]$ of 38.3 and 37.3, respectively; for definition of terms, refer to the footnote of Table 2. Mean air temperature (T) and D provided weaker control on tree H (Table 2). Variables SOL and BA had no impact on the calculation of static H . In all instances, modelled abiotic variables related to H and H_{\max} in a nonlinear manner, giving both positive and negative responses to a monotonic increase in the variables.

The fully parameterised Eq. (8) was able to explain about 67.3% of target plot-level annual mean D -growth, with $\text{RMSE} = 0.13$ and $\text{MAE} = 0.10 \text{ cm years}^{-1}$. For the relative impact of the various predictor variables in the rate equation, consult Table 2. Equation (8)'s expansion by means of symbolic regression generated an expression of cumulated

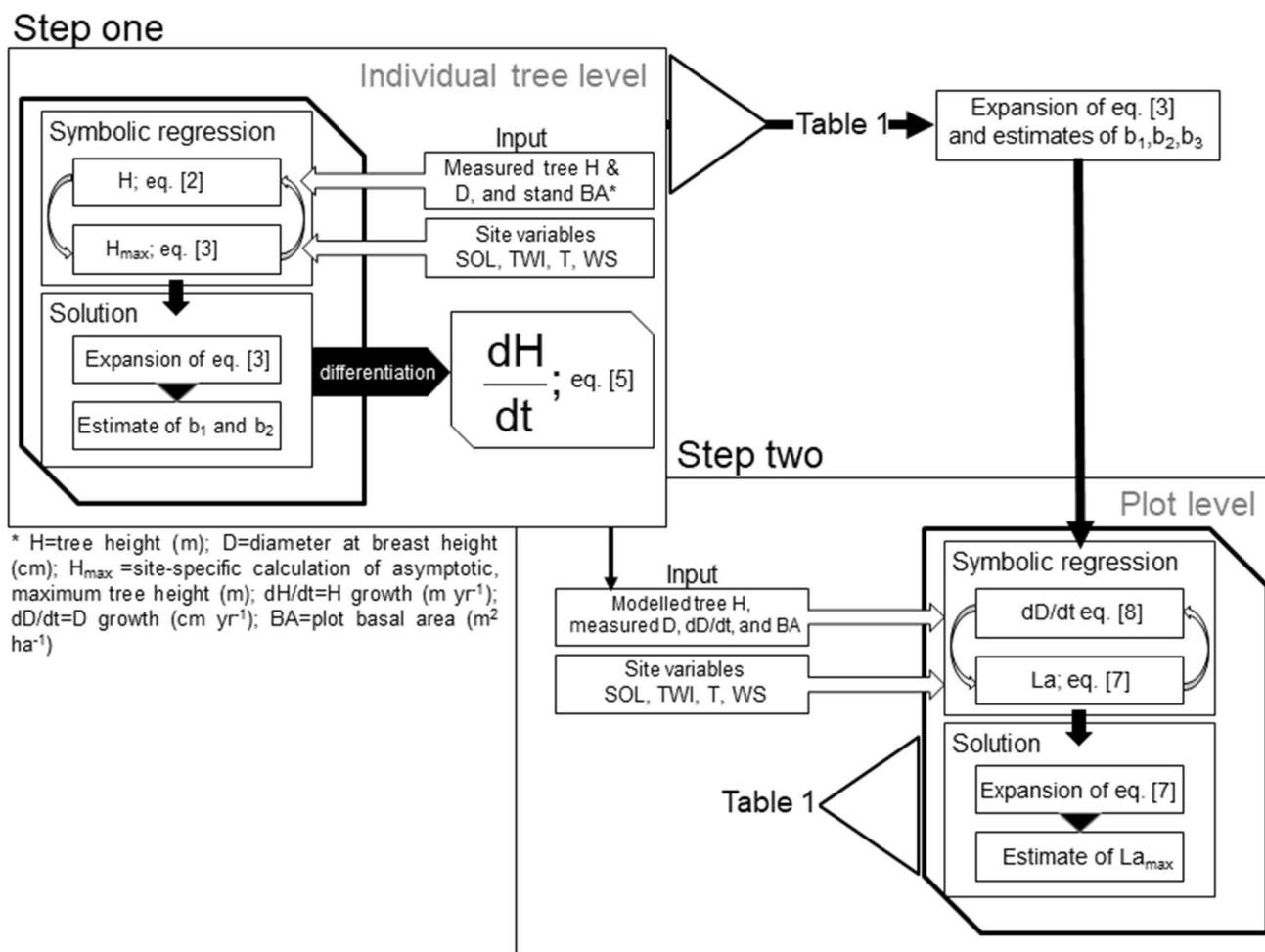


Fig. 4 Equation development process and information flow. Steps one and two of the process coincide with the development of the tree H -rate equation first, followed by the development of the D -rate equation. The H -rate equation is developed from individual-tree data and

the D -rate equation from plot-level data. Information from step one, particularly values for b_1 , b_2 and b_3 and the symbolic expansion of Eq. (3) (Table 1), is passed on to step two in the derivation of the D -rate equation

leaf area (Table 1; Fig. 4). The cumulated leaf area function (i.e. La) is central to the assessment of cumulated leaf area of beech trees as their stems vary in size and shape.

Impact of biotic variables on H growth

Maximum tree H , i.e. H_{max} , is important here, because like *site index* in traditional tree-growth studies, it provides species-specific information regarding the photosynthetic capacity of trees (Thomas and Bazzaz 1999) and the asymptotic maximum H (i.e. growth potential) achievable under specific site conditions and site quality (Oliver and Larson 1996). Site index, in its conventional usage, is defined as the tree H one could anticipate at a specific reference age (e.g. 50 or 100 years) inferred from tree measurements (Weiskittel et al. 2011). Like its counterpart, H_{max} integrates basic physiological information of tree growth as a function of site quality (Weiskittel et al. 2011). In the symbolic expansion

of H_{max} , it is clear that the maximum H of individual trees is exclusively controlled by the abiotic variables at individual tree sites (Table 2). Collectively, the abiotic variables were able to explain roughly 87% of the variation in static tree H (Tables 1, 2). Height in dominant trees tends to grow in a predictable fashion over a wide range of stand densities (Oliver and Larson 1996) and, as a result, variations in the current stand densities (i.e. ca. 200–700 stems per ha, averaging 298 ± 124 stems per ha^{-1}) were altogether inadequate to evoke a noticeable influence on H -growth patterns under the current forest conditions.

Impact of abiotic variables on H – D change

In general, beech trees in areas of high wind velocities ($> 10\ m\ s^{-1}$) and low TWI (< 3 , indicative of lower soil moisture), particularly along ridges, tend to promote the growth of shorter, wider-stemmed trees. The taller,

Table 1 Function definition for variable individual-tree maximum height (H_{max}) in Eq. (2) [expansion of Eq. (3)] and plot-level mean cumulated leaf area (La) in Eq. (8) determined by means of nonlinear

symbolic regression. Also specified are the equation coefficients of the coupled system of differential equations (e.g. G , D_{max} , La_{max} and b_i , where $i = 1, \dots, 4$) set a priori or during regression

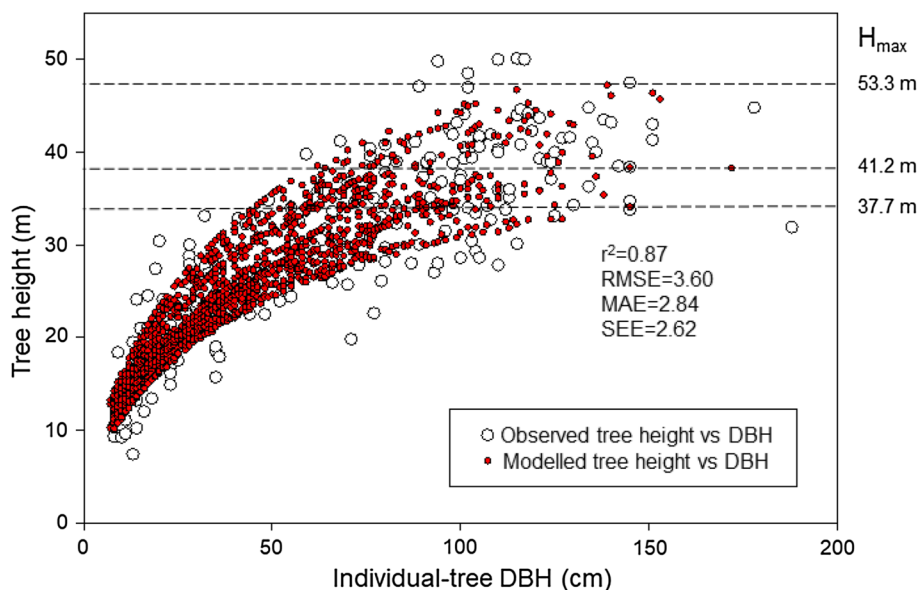
| Dependent variable | Equation components ^a and coefficients |
|----------------------------|---|
| H_{max} (m) | $b_3 \cdot \text{logistic} \left\{ 1.32 \cdot a \tan 2(\text{TWI}, 4) \cdot \cos [4.57 \times 10^4 \cdot \min(0.742\text{TWI}, \text{WS})] \cdot \min \left[\begin{array}{l} \cos \left(\cos \left(\frac{T}{\min(\text{WS}^2 \cdot a \tan 2(\text{TWI}, 4), \text{WS})} \right) \right) \right. \\ \left. \cos [-3.42 \times 10^3 \max(\max(1.65\text{TWI}, \text{WS}), T)] \right] \right\}, \text{ and}$ |
| Leaf area (m^2) | $La_{max} \cdot \text{logistic} \left\{ \text{sqrt} \left[\frac{-5278.5}{D \cdot \min(D, \text{WS} \cdot \text{BA})} + \min(D, 65.2 + \text{BA}) + \max(40, T\sqrt{\lambda}) \right] - \min \left(\begin{array}{l} 0.126\text{WS} \cdot \text{BA} + \max(\text{SOL} - \text{WS}, \text{BA}), \\ 0.55D \end{array} \right) - 12.6 \right\}, \text{ and}$ |
| | $\lambda = H - 1.3 \text{ m}, G = 1100.0 \text{ cm}^3 \text{ m}^{2b}, D_{max} = 200.0 \text{ cm (maximum possible DBH)}^b, La_{max} = 12,647 \text{ m}^{2c}, b_1 = 0.062^c, b_2 = 0.702^c,$ and $b_3 = 74.1 \text{ m}^c$ |

^a $\text{atan}^2(y,x)$ is the two-argument arctangent function, i.e. $\tan^{-1}(y/x)$; output from the logistic function (i.e. $f(x) = 1.0/[1.0 + \exp(-x)]$) varies from 0.0 to 1.0 as site conditions (i.e. TWI, T and WS in the H_{max} equation) and mean plot-forest state (D , H and BA in the leaf-area equation) vary from optimal to sub-optimal; SOL=daily mean incident solar radiation ($\text{kJ m}^{-2} \text{ day}^{-1}$), TWI=SAGA-based calculation of topographic wetness index (unitless), T =growing-season mean air temperature ($^{\circ}\text{C}$), WS=near-surface wind velocity (m s^{-1}), D =diameter at breast height (cm), H =total tree height (m) and BA=basal area ($\text{m}^2 \text{ ha}^{-1}$)

^bConstants set according to current field data and field measurements reported in Smith (1998) for American beech (*Fagus grandifolia* Ehrh.) and sugar maple (*Acer saccharum* Marsh.)

^cCoefficients set during regression

Fig. 5 Comparative graph of modelled and measured individual-tree H 's (in m) as a function of stem DBH (D , in cm). Asymptotic, maximum tree H (i.e. H_{max}) for three sample calculations is indicated to the right of the graph. High values are assigned to sites of favourable growing conditions with respect to available soil water, represented here as a SAGA-based calculation of topographic wetness index (TWI), wind velocity (WS) and mean air temperature (T); lower values are assigned to lower-quality sites



slimmer beech trees and their associated growing environment tend to occur in parts of the landscape closest to sources of water, such as along streams and close to vernal pools, which regularly fill up with water during the snow-melt season. The vernal pools in Fig. 6b are illustrated by light brownish patches in the upper landscape with $\text{TWI} \sim 16$ and low prevailing wind velocities $< 3 \text{ m s}^{-1}$. Spring wetting of the well-drained soils and low-to-moderate wind velocities in the high-elevation parts of the landscape provide favourable growing conditions for oriental beech, causing H -growth in the trees concerned to

increase relative to their radial growth (Fig. 7). This allometric relationship in vicinity to vernal pools is reflected in low ΔD 's (Fig. 2b), high H_{max} 's ($\geq 47.0 \text{ m}$; Fig. 6) and high $\Delta H:\Delta D$ ratios (dH/dD in Fig. 7). Allometric patterns observed in this study are consistent with those reported in Fulton (1999), King et al. (2009), Watt and Kirschbaum (2011), Thomas et al. (2015), Trouvé et al. (2015), Navroodi et al. (2016) and Kalbi et al. (2018) for other tree species growing in different parts of the world.

Table 2 Relative impact of independent variables (x 's) in the calculation of individual-tree height (H) for 2003 and mean annual diameter at breast height increment (i.e. dD/dt) in oriental beech over a 9-year growing period (i.e. 2003–2012). Independent variables are ordered

| Target (dependent) variable | Independent variable | Equation sensitivity ^a | % Positive impact ^b | % Negative impact ^c |
|---|--|--|--|--|
| | | $\frac{\sum_{i=1}^{i=n} \partial z / \partial x_i }{n} \cdot \frac{\sigma(x)}{\sigma(z)}$ | $\frac{\partial z}{\partial x} \geq 0$ | $\frac{\partial z}{\partial x} \leq 0$ |
| Tree height (H ; m) | Wind speed (WS; m s^{-1}) | 38.26 | 52 | 48 |
| | SAGA-based calculation of topographic wetness index (TWI; unitless) | 37.28 | 49 | 51 |
| | Mean air temperature (T ; $^{\circ}\text{C}$) | 9.61 | 55 | 45 |
| | Diameter at breast height (D ; cm) | 1.05 | 100 | 0 |
| | Basal area (BA; $\text{m}^2 \text{ha}^{-1}$) | – | – | – |
| DBH-growth (dD/dt ; cm year^{-1}) | Mid-growing-period solar radiation (SOL; kJ m^{-2}) ^d | – | – | – |
| | Wind speed (WS; m s^{-1}) | 7.73 | 48 | 52 |
| | Mean air temperature (T ; $^{\circ}\text{C}$) | 6.71 | 64 | 36 |
| | SAGA-based calculation of topographic wetness index (TWI; unitless) | 6.43 | 49 | 51 |
| | Diameter at breast height (D ; cm) | 0.91 | 95 | 5 |
| | Basal area (BA; $\text{m}^2 \text{ha}^{-1}$) | 0.36 | 17 | 83 |
| | Tree height (H ; m) | 0.16 | 76 | 24 |
| Mid-growing-period solar radiation (SOL; kJ m^{-2}) | 0.002 | 0 | 100 | |

^aRelative impact that independent variables (x 's) have on the calculation of the target variable, z ; $\sigma(x)$ and $\sigma(z)$ are the standard deviations of x and z for all input data and “ n ” is the total number of data points

^bLikelihood that increasing the independent variable will increase the target variable, unless $\partial z / \partial x = 0$

^cLikelihood that increasing the independent variable will decrease the target variable, unless $\partial z / \partial x = 0$

^dThe independent variable has no role in the calculation of the dependent (target) variable at the individual tree or plot level (i.e. H and dD/dt , respectively)

Cumulated leaf area

Figure 8a provides the modelled cumulated leaf area of oriental beech compared to measured leaf area of hardwood trees harvested in northern Cape Breton Island, Nova Scotia, Canada, and two oriental beech tree from the Kheyrud forest. In general, the shape of the cumulated leaf area curve, especially for smaller D trees (from 7 to 80 cm), is best displayed as a power function of D , or more specifically, leaf area (m^2) = $0.099 \times D^{1.90}$, with a coefficient of determination (r^2) of 0.67, when all data were included (Fig. 8a). This power function is consistent with literature descriptions of cumulated leaf area in other forest systems, e.g. Vertessy et al. (1995). For larger D trees (≥ 80 cm), however, the cumulated leaf area becomes more unpredictable as a simple function of D alone, as the equation for cumulated leaf area in Table 1 illustrates. Environmental site variables become more important to cumulated leaf area as trees become larger.

from most to least important in the calculation of target variables (column 3). Height in trees without height measurements are estimated from Eq. (2) and H_{max} , derived with the equation in Table 1

Relationship between static H - D and ΔH - ΔD

Figure 8b displays the relationship between calculated $H:D$ ratios at the end of the 9-year growing period (starting from 2003) as a function of D . In general, $H:D$ ratios are largest when tree D is smallest (Fulton 1999). This basic property also holds true for $\Delta H:\Delta D$ ratios (data not shown). In general, these trends are reinforced by Sumida's (2015) commentary regarding Trouvé et al. (2015) research in H -growth to D -growth interactions. These relationships ($r^2 = 0.77$, for $H:D$ ratios as a function of D) reflect the asymptotic property of tree measurements as tree size increases.

Figure 9 displays a strong linear relationship between $H:D$ and $\Delta H:\Delta D$ at the end of the 9-year growing period; $r^2 = 0.97$ and associated p values < 0.05 . This association suggests that the defining function between ΔH and ΔD is also asymptotic in nature, similar to the curvilinear relationship between H and D (Fig. 5) and consistent with the asymptotic relationship proposed by Trouvé et al.'s

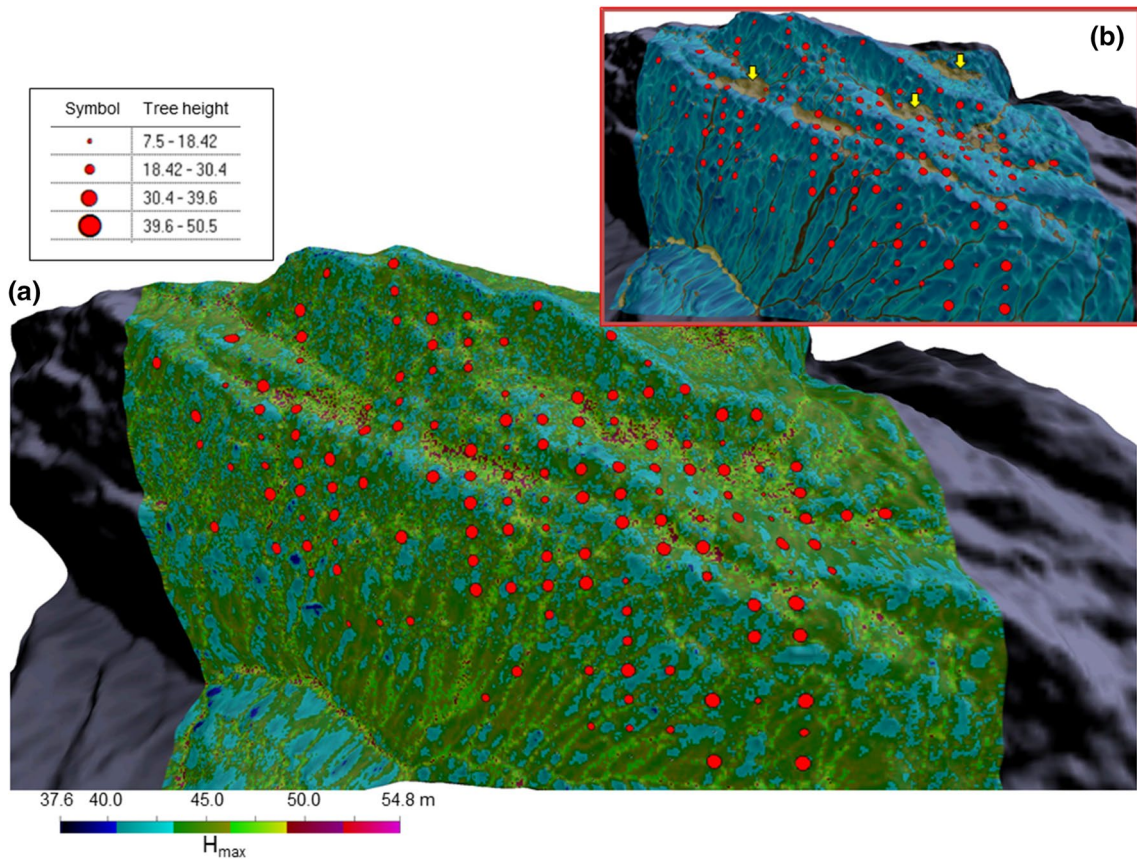
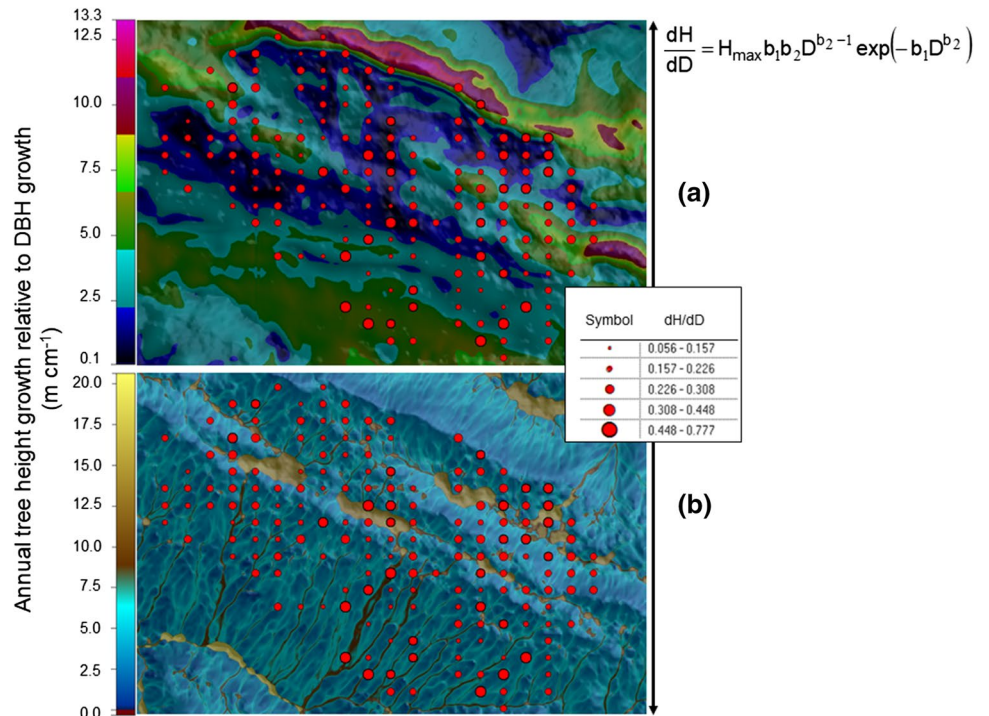


Fig. 6 Individual-tree H 's (red symbols of various sizes) overlain on a map of pixel-based (site) calculations of H_{max} 's (Table 1) for the plot-network-area in the Gorazbon section forest (a); the different colours correspond to variations in H_{max} (legend). The inset b depicts the

same tree H data, but overlain a map of topographic wetness index (TWI). Light brown patches identified by the yellow arrows are land depressions (vernal pools) that collect water during the snowmelt season. (Color figure online)

Fig. 7 Ratio of $\Delta H:\Delta D$ (red symbols of various sizes, legend) superimposed on maps of wind velocity (a) and topographic wetness index (TWI; b). In matching variation in wind velocity and TWI to colours on the maps, refer to the legend to the left of each map. (Color figure online)



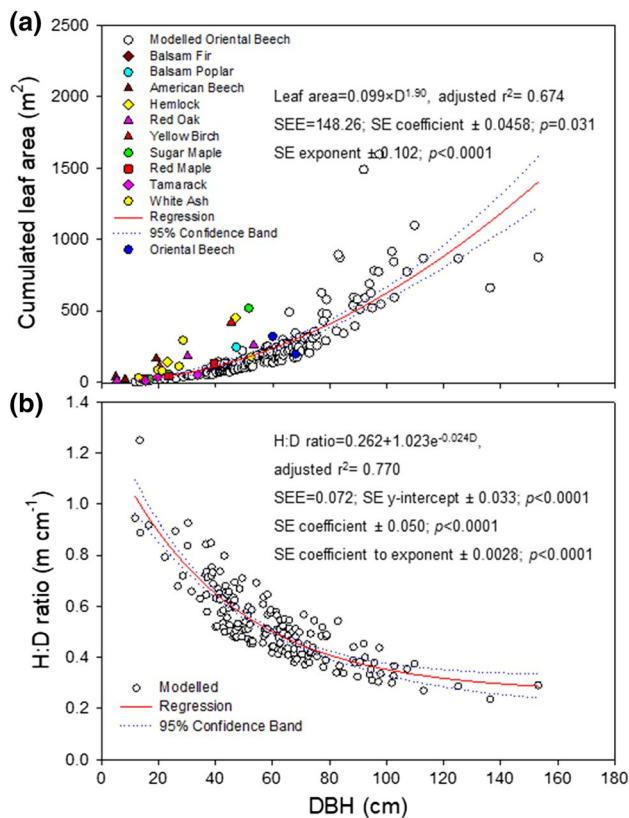


Fig. 8 Modelled and observed cumulated leaf area for oriental beech (m²) compared to observed leaf area for ten hardwood species from northern Cape Breton Island, Nova Scotia, Canada (a), and $H:D$ ratio for oriental beech after 9 years of simulated growth (m cm⁻¹) as a function of D (b). Scientific names of hardwood species not already mentioned in the body of the paper, include: *Abies balsamea* (balsam fir); *Populus balsamifera* (balsam poplar); *Tsuga canadensis* (hemlock); *Quercus rubra* (red oak); *Betula alleghaniensis* (yellow birch); *Larix laricina* (tamarack, larch); and *Fraxinus Americana* (white ash)

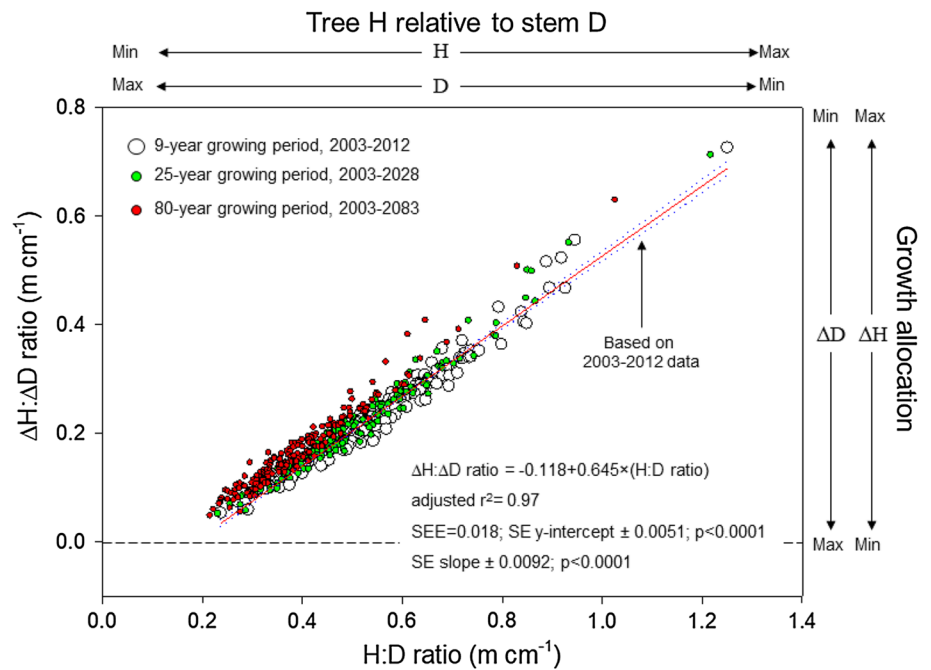
(2015) in their analysis of growth dynamics in sessile oak (*Quercus petraea* Liebl.; Sumida 2015). This relationship seems to maintain over the different time-integration periods (i.e. 9, 25 and 80 years) of this study (Fig. 9). Minor counterclockwise rotation of the nearly linear data clouds for the different time-integration scenarios may reflect inaccuracies caused by error propagation with long-term calculations. This error propagation may be an artefact of the less than perfect equations used to simulate the long-term interactions between static $H-D$ and $\Delta H-\Delta D$. Despite the small inaccuracies, the coupled system of differential equations provides a direct linkage between static $H-D$ and $\Delta H-\Delta D$ relationships. The system also allows incorporation of site quality (abiotic variables, under the

current forest conditions) as an influential feature in the computation of H - and D -growth dynamics in both space and time.

Conclusions

The current paper presents a semi-empirical formulation of a coupled system of differential equations for the assessment of biophysical controls in the allocation of tree growth to tree H -growth and stem D -growth in an unmanaged oriental beech forest in northern Iran. The coupled system relates H and D -increment in oriental beech to plot values of computer-generated abiotic and field-based biotic variables, with an ability to explain about 87 and 67% of the variability in individual-tree and plot-level measurements and related variables. Analysis of equation sensitivity to the various input variables shows that changes in beech H and D are mostly controlled by abiotic factors, particularly wind and soil water content, through TWI. Large, mature trees are shown to grow more slowly, regardless of site variables. Observed patterns in growth allocation to tree H and radial growth relate to the asymptotic nature of both static H to D and H - to D -growth relationships. Intra- and interspecific competition (modelled as a simple function of BA) exerts some level of control, especially with respect to D -increment, but its impact on H -growth is completely nonexistent relative to the impact of abiotic site variables. Reduced H -growth and increased D -growth (small $H:D$ ratios) is observed more frequently in areas of the landscape with high wind velocities, particularly in windward and high-elevation parts of the study area (e.g. ridges), where drier soils predominate. Improved tree H -growth and reduced D -growth (yielding high $H:D$ ratios) is more common in parts of the landscape with high soil water content, particularly in large, seasonally saturated depressions in the landscape (i.e. vernal pools) and where wind velocities are low. These results are consistent with the results in other studies of tree growing patterns in irregular terrain with variable site conditions. On the whole, changes in tree H relative to changes in stem D (i.e. $\Delta H:\Delta D$ ratio) form a strong linear relationship with static tree H and stem D ($H:D$ ratio; $r^2 > 0.97$). The coupled system of differential equations described in this paper is sufficiently general to address the growing patterns of other tree species and forest-development patterns in other forested regions of the world by adapting expressions of potential tree H (by way of H_{\max}) and cumulated leaf area through symbolic regression. This type of work is strongly supported by the need to understand tree growth as it varies in both space and time, especially in view of the current forest-management needs and global climate change.

Fig. 9 Tree H change relative to stem D change (i.e. $\Delta H:\Delta D$ ratio) as a function of static $H:D$ ratio based on tree-growth simulations over 9-, 25- and 80-year growing periods based on the integration of the coupled system of differential equations (Eqs. 5 and 8 after full expansion) with a fourth-order Runge–Kutta procedure and an 0.00125-year timestep



Acknowledgements We are particularly grateful to: (1) D. Edwin Swift formerly of the Canadian Wood Fibre Centre, Canadian Forest Service-Atlantic Forestry Centre, Natural Resources Canada, Fredericton, New Brunswick, Canada, for his comprehensive examination of the original manuscript with respect to both its scientific content and presentation; (2) the Natural Resources Faculty, University of Tehran, Karaj, Iran, for use of the Kheyrod experimental forest and for logistical support to MB; (3) the Ecology and Environmental College, Inner Mongolia Agricultural University, Hohhot, Inner Mongolia, China, in support of CZ's participation in this work; and (4) the Faculty of Forestry and Environmental Management, University of New Brunswick, New Brunswick, Canada, for computer resources and relevant modelling, plotting, and GIS software. We also acknowledge the US National Aeronautics and Space Administration for providing SRTM Plus V3 data free of charge.

References

- Ahmadi K, Alavi SJ (2013) Generalized height-diameter models for *Fagus orientalis* Lipsky in Hyrcanian forest, Iran. *J For Sci* 25:45. <https://doi.org/10.17221/51/2016-jfs>
- Ahmadi K, Alavi SJ, Kouchaksaraei MT, Aertsen W (2013) Non-linear height-diameter models for oriental beech (*Fagus orientalis* Lipsky) in the Hyrcanian forests, Iran. *Biotechnol Agron Soc Environ* 17(3):431–440
- Ashraf MI, Zhao Z, Bourque CPA, Meng FR (2012) GIS evaluation of two slope calculation methods regarding their suitability in slope analysis using high precision LiDAR digital elevation models. *Hydrol Process* 26(8):1119–1133
- Ashraf MI, Bourque CPA, MacLean DA, Erdle T, Meng FR (2013) Estimation of potential impacts of climate change on growth and yield of temperate tree species. *Mitig Adapt Strateg Global Change* 22:4124. <https://doi.org/10.1007/s11027-013-9484-9>
- Austin MP, Pausas JG, Nicholls AO (1996) Patterns of tree species richness in relation to environment in southeastern New South Wales, Australia. *Aust J Ecol* 21:154–164
- Baah-Acheamfour M, Bourque CPA, Meng FR, Swift DE (2013) Classifying forestland from model-generated tree species habitat suitability in the Western Ecoregion of Nova Scotia, Canada. *Can J For Res* 43(6):517–527
- Bang C, Sabo JL, Faeth SH (2010) Reduced wind speed improves plant growth in a desert city. *PLOS ONE* 5:e11061. <https://doi.org/10.1371/journal.pone.0011061>
- Banin L, Feldpausch TR, Phillips OL, Baker TR, Lloyd J et al (2012) What controls tropical forest architecture? Testing environmental, structural and floristic drivers. *Global Ecol Biogeogr* 21:1179–1190
- Bayat M, Pukkala T, Namiranian M, Zobeiri M (2013) Productivity and optimal management of the uneven-aged hardwood forests of Hyrcania. *Eur J For Res* 132:5. <https://doi.org/10.1007/s10342-013-0714-1>
- Bayramzadeh V, Attarod P, Ahmadi MT, Ghadiri M, Akbari R et al (2012) Variation of leaf morphological traits in natural populations of *Fagus orientalis* Lipsky in the Caspian forests of Northern Iran. *Ann For Res* 55(1):33–42
- Becker P, Meinzer FC, Wullschlegler SD (2000) Hydraulic limitation of tree height: a critique. *Funct Ecol* 14:4–11
- Beven K (1997) TOPMODEL: a critique. *Hydrol Process* 11:1069–1085
- Bonan G (2008) *Ecological climatology: Concepts and applications*, 2nd edn. University Press, Cambridge
- Botkin DB (1993) *Forest dynamics: ecological model*. Oxford University Press, New York
- Botkin DB, Janak JF, Wallis JR (1972) Some ecological consequences of a computer model of forest growth. *J Ecol* 60(3):849–872
- Bourque CPA, Bayat M (2015) Landscape variation in tree species richness in northern Iran forests. *PLOS ONE* 10:e0121172
- Bourque CPA, Gullison JJ (1998) A technique to predict hourly potential solar radiation and temperature for a mostly unmonitored area in the Cape Breton Highlands. *Can J Soil Sci* 78:409–420
- Bourque CPA, Meng FR, Gullison JJ, Bridgland J (2000) Biophysical and potential vegetation growth surfaces for a small watershed in northern Cape Breton Island, Nova Scotia, Canada. *Can J For Res* 30(8):1179–1195

- Byun JG, Lee WK, Kim M, Kwak DA, Kwak H et al (2013) Radial growth response of *Pinus densiflora* and *Quercus* spp. to topographic and climatic factors in South Korea. *J Plant Ecol* 6(5):380–392
- Conrad O, Bechtel B, Bock M, Dietrich H, Fischer E, Gerlitz L, Wehberg J, Wichmann V, Böhner J (2015) System for automated geoscientific analyses (SAGA) v. 2.1.4. *Geosci Model Devel* 8:1991–2007
- Coomes DA, Allen RB (2007) Effects of size, competition and altitude on tree growth. *J Ecol* 95:1084–1097
- Detto M, Muller-Landau HC, Mascaro J, Asner GP (2013) Hydrological networks and associated topographic variation as templates for the spatial organization of tropical forest vegetation. *PLOS ONE* 8:e76296. <https://doi.org/10.1371/journal.pone.0076296>
- Falster DS, Westoby M (2005) Alternative height strategies among 45 dicot rain forest species from tropical Queensland, Australia. *J Ecol* 93:521–535
- Fulton MR (1999) Patterns in height-diameter relationships for selected tree species and sites in eastern Texas. *Can J For Res* 29:1445–1448
- Geiger R (1965) *The climate near the ground*. Harvard University Press, Cambridge
- Goudriaan J (1977) *Crop micrometeorology: a simulation study*. Centre for Agricultural Publishing and Documentation, Wageningen
- Gruber S, Peckham SD (2008) Land-surface parameters and objects in hydrology. In: Hengl T, Reuter HI (eds) *Geomorphometry*. Elsevier, Amsterdam, pp 171–194
- Harja D, Vincent G, Mulia R, van Noordwijk M (2012) Tree shape plasticity in relation to crown exposure. *Trees* 26:1275–1285
- Hassan QK, Bourque CPA (2009) Potential species distribution of balsam fir based on the integration of biophysical variables derived with remote sensing and process-based methods. *Remote Sens* 1:393–407
- Henry HAL, Aarssen LW (1999) The interpretation of stem diameter-height allometry in trees: biomechanical constraints, neighbour effects, or biased regressions? *Ecol Lett* 2:89–97
- Heyder JC (1986) *Waldbau im wandel*. In: Sauerlander JD (ed) *Silviculture under change*. Verlag, Frankfurt am Main
- Huang JG, Stadt KJ, Dawson A, Comeau PG (2013) Modelling growth-competition relationships in trembling aspen and white spruce mixed boreal forests of western Canada. *PLOS ONE* 289:300. <https://doi.org/10.1371/journal.pone.0077607>
- Huang P, Wana XC, Lieffers VJ (2016) Daytime and nighttime wind differentially affects hydraulic properties and hignomorphogenic response of poplar saplings. *Physiol Plant* 157:85–94
- Hubbard RM, Bond BJ, Ryan MG (1999) Evidence that hydraulic conductance limits photosynthesis in old *Pinus ponderosa* trees. *Tree Physiol* 19:165–172
- Jaafari A, Najafi A, Zenner EK (2014) Ground-based skidder traffic changes chemical soil properties in a mountainous Oriental beech (*Fagus orientalis* Lipsky) forest in Iran. *J Terramech* 55:39–46
- Jaafari A, Zenner EK, Pham BT (2018) Wildfire spatial pattern analysis in the Zagros Mountains, Iran: A comparative study of decision tree based classifiers. *Ecol Inform* 43:200–211
- Jiang LB, Ye MX, Zhu S, Zhai Y, Xu M et al (2016) Computational identification of genes modulating stem height–diameter allometry. *Plant Biotechnol J* 14:1–11
- Kahnamoie MHM (2003) *The relation between annual diameter increment of Fagus orientalis and environmental factors (Hyrcanian forest-Iran)*. Unpublished MSc, Natural Resources Management, International Institute for Geo-information Science and Earth Observation, the Netherlands
- Kalbi S, Fallah A, Bettinger P, Shataee S, Yousefpour R (2018) Mixed-effects modeling for tree height prediction models of Oriental beech in the Hyrcanian forests. *J For Res* 29(5):1195–1204. <https://doi.org/10.1007/s11676-017-0551-z>
- Kimmins JP (1997) *Forest ecology: a foundation for sustainable management*, 2nd edn. Prentice Hall, Upper Saddle River
- King DA, Davies SJ, Tan S, Noor NS (2009) Trees approach gravitational limits to height in tall lowland forests of Malaysia. *Funct Ecol* 23:284–291
- Koch GW, Sillett SC, Jennings GM, Davis SD (2004) The limits to tree height. *Nature* 428:851–854
- Lebourgeois F, Bréda N, Ulrich E, Granier A (2005) Climate-tree-growth relationships of European beech (*Fagus sylvatica* L.) in the French permanent plot network (RENECOFOR). *Trees* 19:385–401. <https://doi.org/10.1007/s00468-004-0397-9>
- Leibundgut H (1983) Führen naturnahe waldbauverfahren zur betriebswirtschaftlichen erfolgsverbesserung? Do close to nature forestry practices lead to economic improvement? *Forstarchiv* 54:47–51
- Lopes AMG (2003) WindStation: A software for the simulation of atmospheric flows over complex topography. *Environ Model Softw* 18:81–96
- Lutgens FK, Tarbuck EJ (1998) *The atmosphere: an introduction to meteorology*, 7th edn. Prentice Hall, Upper Saddle River
- Maathuis BHP (2006) Digital elevation model based hydro-processing. *Geocarto Int* 21(1):21–26
- Marvie-Mohadjer MR (2012) *Silviculture*. University of Tehran Press, Tehran
- Meng SX, Lieffers VJ, Reid DEB, Rudnicki M, Silins U (2006) Reducing stem bending increases the height growth of tall pines. *J Exp Bot* 57(12):3175–3182
- Merriam JB (1992) Atmospheric pressure and gravity. *Geophys J Int* 109:488–500
- Mohammadi Z, Mohammadi Limaee S, Lohmander P, Olsson L (2018) Estimation of a basal area growth model for individual trees in uneven-aged Caspian mixed species forests. *J For Res* 29(5):1205–1214
- Namiranian M (2009) *Forest management project of Gorazbon section: university of Tehran's Kheyroud experimental forest in northern Iran*. Unpublished Report, Department of Forestry, Faculty of Natural Resources, University of Tehran, Karaj, Iran, 440 p
- Navroodi IH, Alavi SJ, Ahmadi MK, Radkarimi M (2016) Comparison of different non-linear models for prediction of the relationship between diameter and height of velvet maple trees in natural forests (Case study: Asalem Forests, Iran). *J For Sci* 62(2):65–71
- Nilsen ET, Orcutt DM (1996) *Physiology of plants under stress: Abiotic factors*. Wiley, New York
- Oliver CD, Larson BC (1996) *Forest stand dynamics*. Wiley, New York
- Otto HJ (1993a) *Der dynamische walld-ökologische grundlagen des naturnahen waldbaues (The dynamic forest-ecological basis of close to nature forestry)*. *Forst und Holz* 48:331–335
- Otto HJ (1993b) *Waldbau in Europa: Seine schwachen und vorzuge-in historischer perspektive*. *Forestry in Europe: Its weaknesses and strengths-in a historical perspective*. *Forst und Holz* 48:235–237
- Patry C, Kneeshaw D, Wyatt S, Grenon F, Messier C (2013) Forest ecosystem management in North America: from theory to practice. *For Chron* 89(4):525–537
- Poorter L, Bongers L, Bongers F (2006) Architecture of 54 moist-forest tree species: traits, trade-offs, and functional groups. *Ecology* 87(5):1289–1301
- Retuerto R, Woodward FI (1992) Effects of wind speed on the growth and biomass allocation of white mustard *Sinapis alba* L. *Oecologia* 92:113–123
- Ryan MG, Yoder BJ (1997) Hydraulic limits to tree height and tree growth. *Biosciences* 47(4):235–242
- Schmidt M, Lipson H (2009) Distilling free-form natural laws from experimental data. *Science* 324:81–85
- Sefidi K, Marvie-Mohadjer MR, Mosandl R, Copenheaver CA (2011) Canopy gaps and regeneration in old-growth oriental beech (*Fagus orientalis* Lipsky) stands, northern Iran. *For Ecol Manag* 262(6):1094–1099

- Smith MJ (1998) An examination of forest succession in the Cape Breton Highlands of Nova Scotia. Unpublished MSc. Thesis, University of New Brunswick, Fredericton
- Smith VC, Ennos AR (2003) The effects of air flow and stem flexure on the mechanical and hydraulic properties of the stems of sunflowers *Helianthus annuus L.* J Exp Bot 54(383):845–849. <https://doi.org/10.1093/jxb/erg068>
- Spurr SH, Barnes BV (1980) Forest ecology, 3rd edn. Wiley, New York
- Sumida A (2015) The diameter growth-height growth relationship as related to the diameter-height relationship. Tree Physiol 35:1031–1034
- Tabari M, Fayaz P, Espahbodi K, Staelens J, Nachtergale L (2005) Response of oriental beech (*Fagus orientalis* Lipsky) seedlings to canopy gap size. Forest 78(4):443–450. <https://doi.org/10.1093/forestry/cpi032>
- Thomas SC, Bazzaz FA (1999) Asymptotic height as a predictor of photosynthetic characteristics in Malaysian rain forest trees. Ecology 80(5):1607–1622
- Thomas SC, Martin AR, Mycroft EE (2015) Tropical trees in a wind-exposed island ecosystem: height-diameter allometry and size at onset of maturity. J Ecol 103:594–605
- Trouvé R, Bontemps J-D, Seynave I, Collet C, Lebourgeois F (2015) Stand density, tree social status and water stress influence allocation in height and diameter growth of *Quercus petraea* (Liebl.). Tree Physiol 35:1035–1046
- Vertessy RA, Benyon RG, O’Sullivan SK, Gribben PR (1995) Relationships between stem diameter, sapwood area, leaf area and transpiration in a young mountain ash forest. Tree Physiol 15:559–567
- Wadsworth RM (1959) An optimum wind speed for plant growth. Ann Bot 23(89):195–199
- Watt MS, Kirschbaum MUF (2011) Moving beyond simple linear allometric relationships between tree height and diameter. Ecol Model 222:3910–3916
- Weiskittel AR, Hann DW, Kershaw JA Jr, Vanclay JK (2011) Forest growth and yield modeling. Wiley, Hoboken
- Willoughby I, Stokes V, Kerr G (2009) Side shelter on lowland sites can benefit early growth of ash (*Fraxinus excelsior* L.) and sycamore (*Acer pseudoplatanus* L.). Forestry. Oxford University Press, Oxford

Publisher’s Note Springer Nature remains neutral with regard to jurisdictional claims in published maps and institutional affiliations.